Proceedings of 5th Jagiellonian Symposium on Advances in Particle Physics and Medicine, Kraków, Poland, 2024

Development of the KAPAE II Detector for New Particle Search in Positronium Decay

D.W. Jeong, H.W. Park and H.J. Kim*

Department of physics, Kyungpook National University, Deahak-ro 80, Deagu 41566, Korea

Doi: 10.12693/APhysPolA.146.679 *e-mail: hongjoo@knu.ac.kr

The positronium annihilation experiment is important for searching for new particles through invisible decay channels. It allows the study of milli-charged particles, mirror worlds, and extra dimensions via totally invisible decay modes, as well as axion-like particles, dark photons, and dark Z bosons through partially invisible decay modes. The Kyungpook National University Advanced Positronium Annihilation Experiment (KAPAE) aims to study positronium annihilation, focusing on both visible and invisible exotic decay processes. The KAPAE phase II detector enhances sensitivity to the invisible decay of positronium by reducing dead areas and optimizing the channel configuration. It is composed of a 5×5 array of bismuth germanate (BGO, $Bi_4Ge_3O_{12}$) scintillation crystals, each measuring $30\times30\times150$ mm^3, resulting in an overall size of approximately $150 \times 150 \times 150$ mm^3. Simulations suggest an upper limit of sensitivity for invisible decay of approximately 2.7×10^{-9} (90% C.L.). This paper presents the optimization, data acquisition system, construction, and performance testing of the KAPAE II detector.

topics: positronium, BGO, silicon photomultiplier (SiPM), invisible decay

1. Introduction

As a pure leptonic system, positronium is composed of an electron and a positron. Accurate measurements of positronium multiphoton decay can be used to test the standard model, search for new particles, and study charge (C), charge-parity (CP), and charge-parity-time reversal (CPT) [1, 2]. Missing energy from positronium annihilation allows for the study of invisible decay search. Models for totally invisible exotic decays include milli-charged particles, extra dimensions, and mirror worlds [3, 4]. Partially invisible exotic decay models, such as axion-like particles (ALP), have a limit in the range of approximately 10^{-4} to 10^{-6} set by several groups. Additionally, dark photons [5] and dark Z bosons [6] are predicted by theory, and these searches are possible with positronium annihilation. Various groups are conducting experiments to study these diverse targets. The J-PET (Jagiellonian positron emission tomography) group [7, 8] and the APEX (A Positron–Electron eXperiment) group [9] have designed cylindrical detectors for CP and CPT violation studies using high angular resolution. Recently, the J-PET group confirmed consistency with quantum electrodynamics (QED) expectations at the 0.0007 level and within one standard deviation [10, 11]. The ETH Zurich [12] group has developed a 4π calorimeter to investigate totally invisible decays. The upper limits on the branching ratios for the totally invisible decay of para-positronium (p-Ps) and ortho-positronium (o-Ps) confirmed by the ETH Zurich group are 4.3×10^{-7} and 4.2×10^{-7}, respectively [13].

The Kyungpook National University Advanced Positronium Annihilation Experiment (KAPAE) aims to observe rare decays of positronium through a compact, tabletop, laboratory-scale experiment. Compared to other previous experiments, the detector is smaller in size, features simpler electronics, and is designed with a modular approach to allow for easy handling, upgrades, and repurposing. We use silicon photomultipliers (SiPMs) and a custom-made data acquisition (DAQ) system coupled with BGO to improve light collection efficiency and energy resolution and significantly reduce the size of the electronics. To ensure high trigger efficiency, instead of using optical fibers, the radioactive source and trigger channel with polyethylene naphthalate (PEN) film plastic scintillator and SiPM are directly embedded at the center of the detector. The KAPAE I detector has been completed, and data analysis is ongoing for the rare decays of ortho-positronium (o-Ps) [14]. The KAPAE I detector is constructed in a rectangular shape with dimensions of $105 \times 105 \times 150$ mm^3 by stacking a 14×14 array of $7.5 \times 7.5 \times 150$ mm^3 bismuth germanate (BGO, Bi4Ge3O_{12}) scintillation crystals coupled with SiPMs. This design utilizes high angular resolution to analyze multiphoton decay events of ortho-positronium.

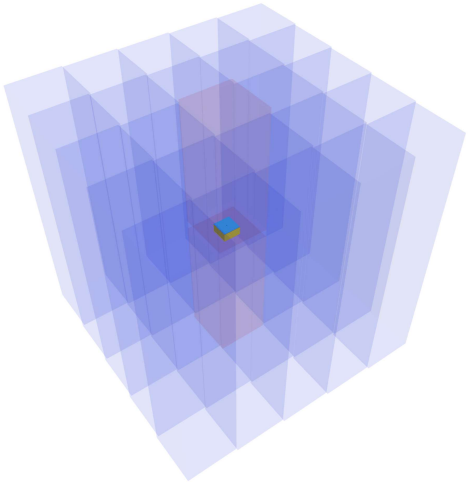

Fig. 1. Schematic representation of the trigger part and gamma detection part of the KAPAE phase II detector.

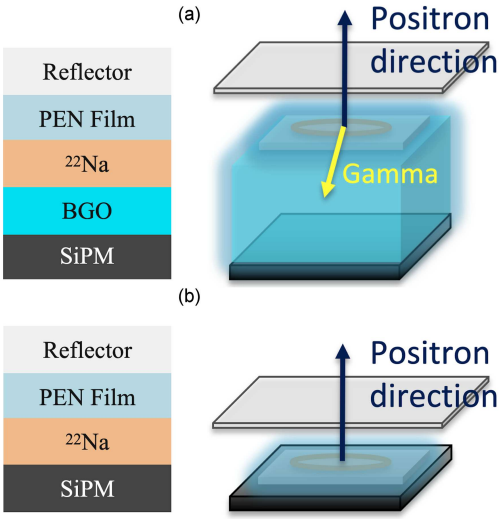

Fig. 2. (a) Schematic representation of the phoswich trigger. (b) Schematic representation of the 1-channel SiPM embedded trigger.

The KAPAE II detector is designed to improve the invisible decay sensitivity of the KAPAE I detector. To reduce dead areas, the number of channels is decreased while the overall size of the detector is increased. Optimization of the BGO scintillation crystal and SiPM enhances the energy resolution. To optimize trigger efficiency and minimize dead areas, two different trigger systems, i.e., the phoswich trigger and a trigger combining SiPM and PEN film are studied.

In this study, we report the optimization and construction of the KAPAE II detector, focusing on invisible decay sensitivity at ground level and room temperature. The detector is constructed in a cubic shape with dimensions of approximately $150 \times 150 \times 150$ mm^3 by stacking a 5×5 array of $30 \times 30 \times 150$ mm^3 BGO scintillation crystals. The KAPAE II detector aims to search for the invisible decay of positroniums, such as ALP, dark photon, and dark Z. Two different trigger systems are studied to improve the sensitivity of the invisible positronium decay.

2. KAPAE II detector

The KAPAE II detector consists of BGO scintillation crystals arranged in a 5×5 array, each measuring $30 \times 30 \times 150$ mm^3, and a positron trigger part. To install the positron trigger, the central BGO crystal is divided into two endcap BGO crystals, each with dimensions of $30 \times 30 \times 75$ mm^3. The space between the two endcap BGO crystals is designed to be adjustable, facilitating upgrades and modifications to the trigger part of the detector. Figure 1 presents a schematic representation of the trigger and gamma detection parts of the KAPAE II detector.

2.1. Design and optimization of the positron trigger part

The KAPAE detector is triggered at the coincidence of a positron and a 1 274 keV gamma ray emitted during the decay of ^{22}Na. The positron trigger part needs to precisely detect the positron emitted at the exact center of the closed detector. Two candidates for the positron trigger are the phoswich trigger and a trigger combining a 1-channel SiPM and PEN film. Both methods use a PEN film plastic scintillator optimized to a thickness of 125 μm in the KAPAE I detector [15].

The phoswich trigger couples a PEN film plastic scintillator with a BGO scintillation crystal, covering them with a reflector and discriminating between the PEN film signal and the BGO signal via pulse shape discrimination (PSD). Figure 2a illustrates the design of this phoswich trigger. The advantage of this method is minimizing the dead area inside the detector, which improves sensitivity. However, due to the fast decay time component of BGO ($\approx$ 45.8 ns for 8%) [16] being insufficiently distinct from the decay time of the PEN film signal ($\approx$ 18 ns), this method was excluded as a candidate in the current setup.

As shown in Fig. 2b, the 1-channel SiPM embedded method involves placing a 1-channel SiPM with dimensions of $6.85 \times 7.35 \times 1.45$ mm^3 inside the detector to directly read the positron signal from the PEN film. Although this method increases the dead area inside the detector due to the additional 1-channel SiPM and signal wires, the preamp is located outside the detector, unlike in KAPAE I, minimizing the dead area. This achieves a high trigger rate and improved reliability. The impact of

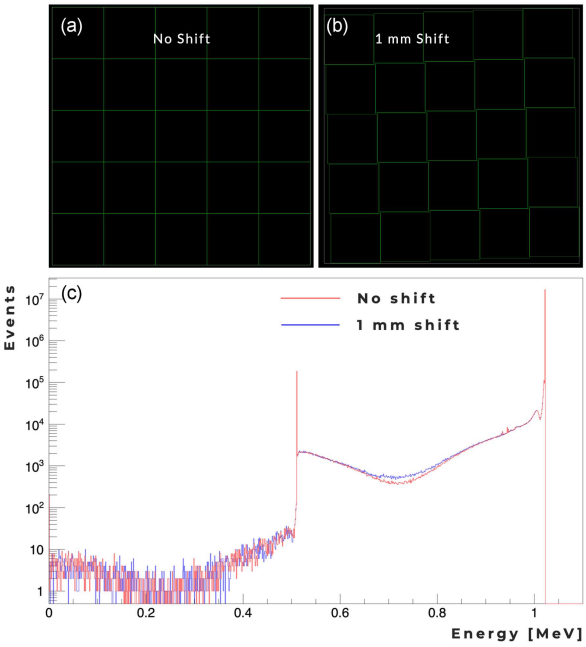

Fig. 3. Geant4 simulation construction of (a) uniformly stacked BGO crystals and (b) 1 mm shifted BGO crystals. (c) Energy deposition histogram from the Geant4 simulation results of the BGO scintillation crystals.

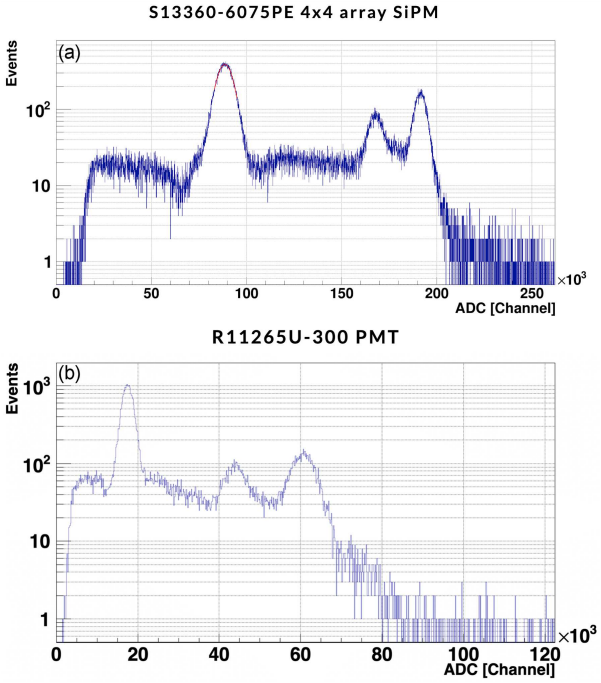

Fig. 4. ^{22}Na gamma pulse height spectrum measured with (a) the S13360-6075PE 4×4 array SiPM and (b) the R11265U-300 PMT.

the dead area of this SiPM embedded method will be evaluated in the subsequent section using the Geant4 Monte Carlo simulations toolkit [17].

2.2. Design and optimization of gamma detection part

Four studies were conducted to optimize the gamma detection part. First, we focused on the dead area, which was arranged by BGO crystal scintillators. During the stacking of the BGO crystals, a 3M enhanced specular reflector (ESR) film was inserted as a reflector between all the BGO crystals. To evaluate the impact of the uniform grid-like dead area created by this arrangement, we conducted simulations using the Geant4 simulation toolkit. We compared two cases, i.e., one with a uniformly stacked arrangement and another with all BGO crystals shifted by 1 mm. Figure 3 shows the simulation results. We compared events where two 511 keV back-to-back gamma rays deposited less than 60 keV in the detector before escaping. Out of 100 million events, 448 were observed in the no-shift case (panel a) and 421 in the 1 mm shift case (panel b), indicating a negligible impact on the detector's sensitivity. Therefore, the detector was designed with a uniform grid arrangement.

Second, a study was conducted to improve the light collection efficiency based on the surface condition of the BGO crystals. Although BGO crystals have high gamma detection efficiency due to their high density and atomic number, their high refractive index of 2.17 causes internal scintillation light to be trapped, resulting in poor light collection efficiency. To address this issue, the four lateral surfaces of 30×150 mm^2 BGO crystals were etched to create diffuse reflection, enhancing light collection efficiency. As a result, the BGO crystals used in the KAPAE phase II detector achieved an average improvement of 22% in light collection efficiency [18].

Third, a study was conducted to compare the performance of photomultiplier tubes (PMTs) and silicon photomultipliers (SiPMs). As the size of the BGO crystals increased, optimization of the photodetectors coupled to the scintillator was necessary. Two photodetectors with high photosensitivity were selected, i.e., the R11265U-300 3×3 cm^2 square PMT and the S13360-6075PE SiPM from Hamamatsu. We compared these photodetectors by coupling them with the BGO scintillation crystal using optical grease (EJ-550) and 3M ESR film as the reflector. The DAQ system for measurements was custom-built by Notice Korea [19], including both the test system and the system for the completed detector.

The energy resolution of the R11265U-300 PMT was 18.2% for 511 keV, while the S13360-6075PE 4×4 array showed an energy resolution of 11.8%, as shown in Fig. 4. One disadvantage of the R11265U-300 PMT is that its photocathode size is 23×23 mm^2, i.e., smaller than the active area

Fig. 5. (a) Front view and (b) back view of the custom 4×4 array SiPM. (c) Preamp directly coupled to the SiPM. (d) Combined view of the array SiPM and preamp. (e) The custom DAQ system capable of connecting up to 64 channels.

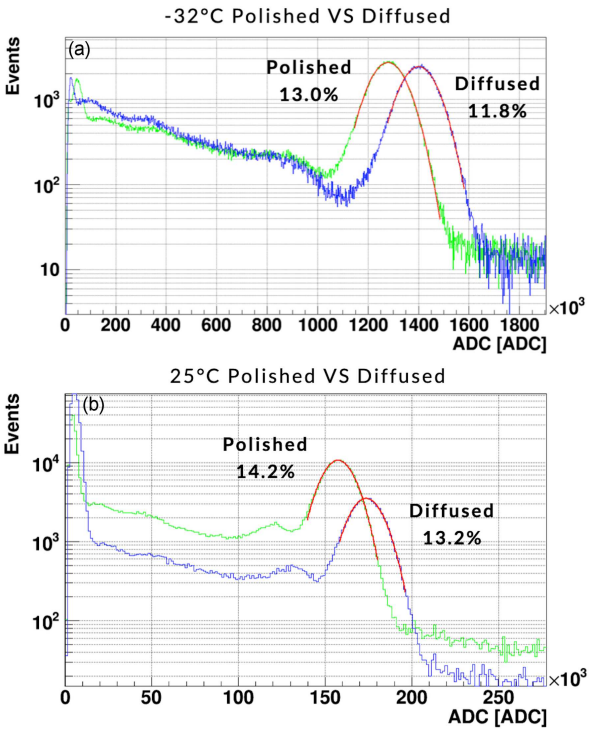

Fig. 6. The 662 keV gamma spectrum of ^{137}Cs measured with SiPM and BGO at room temperature and low temperature.

of the BGO crystal. Considering the overall scale of the electronics and the energy resolution, KAPAE II uses S13360-6075PE SiPMs in a 4×4 array configuration. Figure 5 shows the SiPM, preamp, and DAQ system customized by Notice Korea based on the optimized results. The preamp is designed with variable resistors to adjust the gain of each of the 16 SiPMs in the 4×4 array and is built to connect directly to the SiPMs to minimize noise interference. The custom DAQ, capable of connecting up to 64 channels, is designed to handle positron triggers and 1 274 keV gamma triggers simultaneously. It can record the waveform, charge, mean time, trigger time, peak time, and pulse height.

Fourth, the temperature dependence of light yield, decay time, and energy resolution of SiPMs and BGO scintillation crystals was studied. Energy measurements of 662 keV gamma rays from ^{137}Cs were taken at room temperature (25°C) and low temperature (−32°C). To minimize the impact of moisture, EJ-560 optical pads were used to couple the SiPMs and BGO scintillation crystals. Figure 6 shows the results of these temperature experiments. It was observed that the energy resolution improved by $\approx 10\%$ at low temperatures for both polished and diffused BGO crystals.

2.3. Detector assembly

Figure 7a shows the overall design of the KAPAE II detector. We compared configurations where SiPMs are coupled to both sides of the BGO crystal and where only one side is coupled with the opposite side blocked by a reflector, using 511 keV gamma rays from ^{22}Na. The both-side readout achieved an energy resolution of 11.2%, while the single-side readout achieved a resolution of 12%. Both-side readout requires additional calibration to combine data from both sides. Initially, we use a single-sided readout to simplify data acquisition and analysis, with plans to upgrade to a both-sided readout later.

Figure 7b shows the assembly process of the KAPAE II detector. Each channel is independent to facilitate management and upgrades, and reflectors are assembled to isolate each SiPM to prevent light leakage between channels. Since the central endcap BGO crystals are divided into two parts, an additional SiPM is installed on the opposite side. The detector consists of 27 channels,

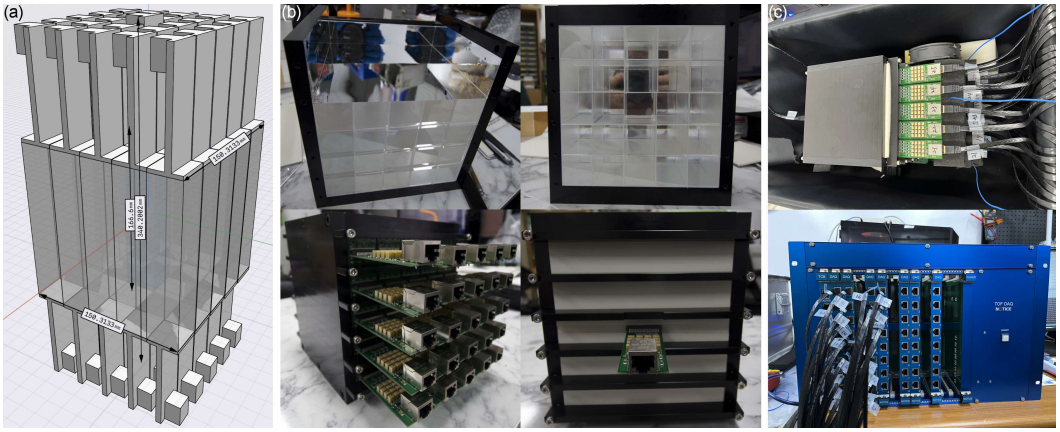

Fig. 7. (a) Schematic representation of the overall KAPAE II detector. (b) Assembly process of the KAPAE II detector. (c) Detector connected to the DAQ system.

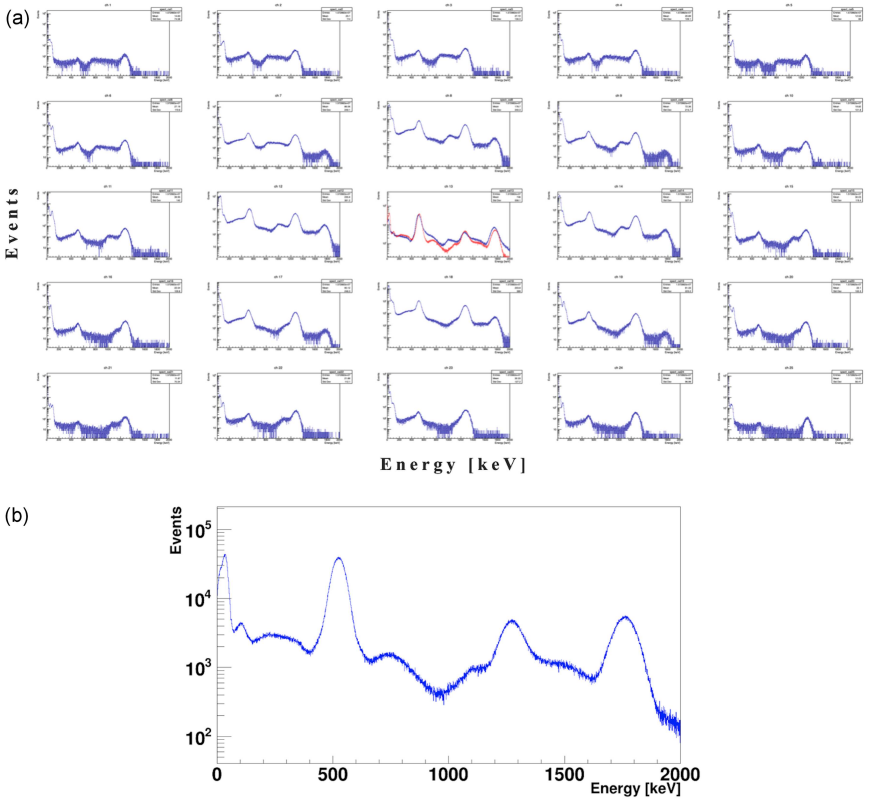

Fig. 8. (a) Calibration results of the KAPAE II detector optimization data to energy. (b) Energy calibration histogram of endcap BGO crystal for channel 13.

including the positron trigger and 26-gamma detection parts. Figure 7c shows the completed detector placed in a dark box connected to the KAPAE II DAQ system.

3. Performance of detector

We are currently measuring the energy of gamma rays produced by the decay of p-Ps at room temperature and ground level. The Geant4 simulation toolkit was used to validate the performance of the designed detector. By simulating the decay of ^{22}Na, we analyzed 2.5×10^8 events where the positron was triggered, and an energy deposition of 1 200 keV or more was observed in the BGO crystal. This data is used to adjust the threshold and calibrate the energy of the KAPAE II detector.

Based on the simulation results, we calibrated the $1.57{\times}10^7$ data points obtained after activating the positron trigger nd the 1 274 keV gamma-ray

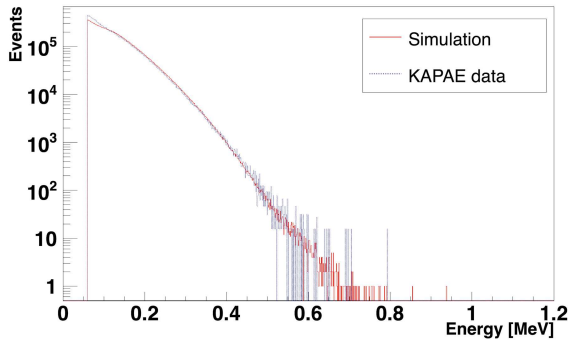

Fig. 9. Comparison of the trigger channel simulation results with actual trigger data.

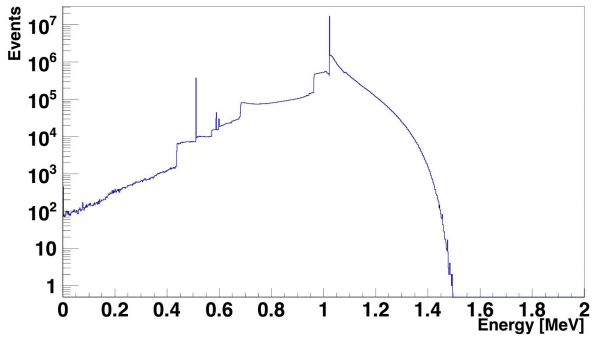

Fig. 10. Simulation results of the energy deposited in the 26 BGO scintillation crystals, excluding the triggered 1 274 keV.

trigger. Figure 8 shows the energy distribution for each of the 26 BGO channels after calibration with the 1 274 keV gamma ray.

Table I shows the energy resolution of 26 BGO channels for the 1 274 keV gamma in the KAPAE II detector. The results indicate an average energy resolution of 7.5% with a standard deviation of 0.4%. Gain adjustment or replacement of the SiPMs in channels 21 and 13-2, which deviate from the average, is planned. For 511 keV measurements, an average energy resolution of $\approx$ 11% was observed, and for ^{137}Cs 662 keV measurements, the average energy resolution was $\approx$ 10%. This demonstrates significant improvement compared to the previous KAPAE I experiment, which showed an energy resolution of 16% at 1 274 keV, and the ETH Zurich experiment, which showed an energy resolution of 15% at 662 keV [20].

Figure 9 shows the energy deposited in the trigger compared with the simulation. The trigger data and simulation results agree well, and the simulation will be used to further optimize the threshold of the trigger channels. Currently, a trigger rate of $\approx$ 25 000 Hz is observed. Once the threshold optimization is completed, the activity of the ^{22}Na radioactive source will be increased to achieve the maximum operating performance of

TABLE I

Energy resolution of 26 BGO channels with 1 274 keV gamma in the KAPAE II detector.

Channel [#]	Energy resolution (FWHM) [%]	Channel [#]	Energy resolution (FWHM) [%]
1	7.4	14	7.5
2	7.7	15	7.7
3	7.8	16	7.5
4	7.3	17	7.4
5	6.7	18	7.5
6	7.6	19	7.6
7	7.3	20	7.6
8	7.2	21	8.4
9	7.6	22	7.6
10	7.2	23	7.7
11	7.8	24	7.3
12	7.4	25	6.8
13-1	6.9	13-2	8.7

the DAQ, targeting a trigger rate of 100 000 Hz, which is much higher than in the previous experiment [13].

Figure 10 shows the simulation results of the total energy deposited in each channel of the detector when the energy exceeds 60 keV. According to the simulation, the number of events with a total energy deposition of less than 60 keV is estimated to be 837 out of 2.5×10^8 simulated events. Based on these events, the upper limit of the totally invisible decay sensitivity in positronium decay is calculated to be 2.7×10^{-9} (90% C.L.) for 90 days of data and 1.3×10^{-9} (90% C.L.) for one year of data, which is 10 to 100 times better sensitivity than the previous results [13].

We will then compare the simulation results with detector data for all channels to analyze invisible decays and obtain the upper limits on the branching ratios for the invisible decay of positronium. In this process, it is necessary to set thresholds according to the energy resolution of each channel and conduct further studies on noise and background. These factors, including energy resolution and thresholds, will be incorporated into the simulation. However, potential systematic errors may arise from the accuracy of the simulation geometry, noise estimation, environmental and cosmic radiation backgrounds, and uncertainties in energy resolution. To minimize these uncertainties, the experiment will be performed in a low-temperature environment to reduce SiPM noise. Additionally, cosmic and environmental radiation backgrounds will be minimized through deep underground operation, radon-free nitrogen flushing, and the use of appropriate shielding.

4. Conclusions

The search for new particles can be performed with the positronium annihilation experiment through invisible decay channels, and several experiments are ongoing. The search for milli-charged particles, mirror dark matter, mirror worlds, and extra dimensions can be performed with totally invisible decay modes, while the search for ALP, dark photons, and dark Z bosons can be performed with partially invisible decay modes.

The KAPAE phase II detector is designed to enhance sensitivity for invisible decay searches. It comprises a 5×5 array of diffused BGO crystals, each measuring $30 \times 30 \times 150$ mm^3, resulting in an overall size of $\approx 150 \times 150 \times 150$ mm^3. The trigger system employs an embedded 1-channel SiPM and PEN film. Using diffused surface BGO scintillation crystals and optimized custom SiPMs, an energy resolution of 7.5% for 1 274 keV has been achieved.

A total of 1.57×10^7 events were used to calibrate the energy of the 26 BGO detector channels and trigger channel. Geant4 simulation was used to estimate the sensitivity to the upper limit of positronium's invisible decay, which is $\approx 2.7 \times 10^{-9}$ (90% C.L.) with three months of data taking.

The KAPAE II detector will operate in a low-temperature environment at -30°C and in the 1000 m deep Yemi Underground Laboratory [21] with copper and lead shielding. The low-temperature environment is expected to improve the detector's minimum detectable energy and energy resolution. Simultaneously, operation in the underground laboratory will reduce cosmic and environmental radioactive background. We aim to search for the invisible decay of p-Ps and o-Ps through these upgrades. With these upgrades, the detector will achieve the world's best sensitivity for detecting invisible decays, allowing us to obtain new upper limits on the branching ratios for the total and partial invisible decays of positronium.

Acknowledgments

This work was supported by the National Research Foundation (NRF) of Korea grant funded by the Korean government (MSIT) (No. 2022R1A6A3A13066208, RS-2024-00348317).

References

[1] K. Dulski, S.D. Bass, J. Chhokar et al., *Nuclear Instruments and Methods in Physics Research Section A: Accelerators, Spectrometers, Detectors and Associated Equipment* **1008**, 165452 (2021).

[2] C. Bartram, R. Henning, D. Primosch, *Nucl. Instrum. Meth. A* **966**, 163856 (2020).

[3] C. Vigo, L. Gerchow, L. Liszkay, A. Rubbia, P. Crivelli, *Phys. Rev. D* **97**(9), 092008 (2018).

[4] C. Vigo, L. Gerchow, B. Radics, M. Raaijmakers, A. Rubbia, P. Crivelli, *Physical Rev. Lett.* **124**(10), 101803 (2020).

[5] J. Pérez-Ríos, S.T. Love, *The European Physical Journal D* **72**, 1 (2018).

[6] D.-W. Jung, K.Y. Lee, C. Yu, *Phys. Rev. D* **105**, 095023 (2022).

[7] P. Moskal, K. Dulski, N. Chug et al., *Science Advances* **7**(42), 4394 (2021).

[8] P. Moskal, B. Jasińska, E.L. Stepień, S.D. Bass, *Nature Reviews Physics* **1**(9), 527 (2019).

[9] C. Bartram, R. Henning, D. Primosch, *Nuclear Instruments and Methods in Physics Research Section A: Accelerators, Spectrometers, Detectors and Associated Equipment* **966**, 163856 (2020).

[10] P. Moskal, E. Czerwiński, J. Raj et al., *Nature Communications* **15**(1), 78 (2024).

[11] P. Moskal, A. Gajos, M. Mohammed et al., *Nature Communications* **12**(1), 5658 (2021).

[12] M.W. Heiss, G. Wichmann, A. Rubbia, P. Crivelli, *Journal of Physics: Conference Series* **1138**(1), 012007 (2018).

[13] A. Badertscher, P. Crivelli, W. Fetscher, U. Gendotti, S.N. Gninenko, V. Postoev, A. Rubbia, V. Samoylenko, D. Sillou, *Phys. Rev. D* **75**, 032004 (2007).

[14] H.W. Park, D.W. Jeong, J. Jegal, A. Khan, H.J. Kim, *Journal of Instrumentation* **18**(03), 03011 (2023).

[15] D.W. Jeong, A. Khan, H.W. Park, J. Lee, H.J. Kim, *Nuclear Instruments and Methods in Physics Research Section A: Accelerators, Spectrometers, Detectors and Associated Equipment* **989**, 164941 (2021).

[16] A. Gonzalez-Montoro, S. Pourashraf, J.W. Cates, C.S. Levin, *Frontiers in Physics* **10**, (2022).

[17] S. Agostinelli, J. Allison, K.a. Amako, J. Apostolakis, H. Araujo, P. Arce, M. Asai, D. Axen et al., *Nuclear instruments and methods in physics research section A: Accelerators, Spectrometers, Detectors and Associated Equipment* **506**(3), 250 (2003).

[18] D. Jeong, J. Cho, E. Choi, L.T. Nguyen, H.J. Kim, *Collection Efficiency of Scintillation Light Depending on Surface Treatment of BGO. Paper presented at the 17th International Conference on Scintillating Materials and their Applications*, University of Milano — Bicocca, Milan, Italy, 8-12 July 2024 (2024).

[19] Notice Korea.

[20] U. Gendotti, *Design of an experiment to search for invisible decays of orthopositronium in vacuum and ortho-positronium formation studies in mesostructured silica films*, PhD thesis, ETH Zurich (2010).

[21] K.S. Park, Y.D. Kim, K.M. Bang, H.K. Park, M.H. Lee, J. So, S.H. Kim, J.H. Jang, J.H. Kim, S.B. Kim, *Frontiers in Physics* **12**, (2024).